Circularly-polarized THz wave emission from a micro-thin water flow

Hsin-Hui Huang
Academia Sinica
Saulius Juodkazis
Swinburne University of Technology https://orcid.org/0000-0003-3897-2844
Eugene Gamaly
Australian National University
Takeshi Nagashima
Setsunan University
Tetsu Yonezawa
Hokkaido University https://orcid.org/0000-0001-7371-204X
Koji Hatanaka (kojihtnk@gate.sinica.edu.tw)
Academia Sinica

Letter

Keywords: THz wave emission, micro-thin water flow, THz science, non-ionizing radiation

Posted Date: September 23rd, 2020

DOI: https://doi.org/10.21203/rs.3.rs-77877/v1

Circularly-polarized THz wave emission from a micro-thin water flow

HSIN-HUI HUANG,[1] SAULIUS JUODKAZIS,[2,3,4,5*] EUGENE G. GAMALY,[6] TAKESHI NAGASHIMA,[7**] TETSU YONEZAWA,[8,9] AND KOJI HATANAKA[1,10,11***]

[1]*Research Center for Applied Sciences, Academia Sinica, Taipei 11529, Taiwan*
[2]*Centre for Micro-Photonics and ARC Training Centre in Surface Engineering for Advanced Materials (SEAM), School of Science, Swinburne University of Technology, Hawthorn, VIC 3122, Australia*
[3]*Currently with the Department of Electronic Journals, The Optical Society (OSA), 2010 Massachusetts Avenue NW, Washington, DC 20036, USA*
[4]*Tokyo Institute of Technology, 2-12-1 Ookayama, Meguro-ku, Tokyo 152-8550, Japan*
[5]*Institute of Advanced Sciences, Yokohama National University, 79-5 Tokiwadai, Hodogaya-ku, Yokohama 240-8501, Japan*
[6]*Laser Physics Centre, Research School of Physics and Engineering, The Australian National University, Canberra, ACT 0200, Australia*
[7]*Faculty of Science and Engineering, Setsunan University, 17-8 Ikeda-Nakamachi, Neyagawa, Osaka 572-8508, Japan*
[8]*Division of Materials Science and Engineering, Faculty of Engineering, Hokkaido University, Hokkaido 060-8628, Japan*
[9]*Institute for the Promotion of Business-Regional Collaboration, Hokkaido University, Hokkaido 001-0021, Japan*
[10]*College of Engineering, Chang Gung University, Taoyuan 33302, Taiwan*
[11]*Department of Materials Science and Engineering, National Dong-Hwa University, Hualien 97401, Taiwan*
**sjuodkazis@swin.edu.au, **t-nagash@mpg.setsunan.ac.jp, ***kojihtnk@gate.sinica.edu.tw*

Intense THz wave sources are highly expected for further progresses in nonlinear THz science and practical implementation of non-ionizing radiation in sensing and communications [1]. Solid-based sources have inherent limits of material breakdown, while intense laser irradiation of liquids is a promising emerging technique for THz wave [2,3] and hard X-ray [4] emission. Water-based THz emission shows intensity enhancements up to 10^3 times when laser-pulse pairs with nanosecond delay are used [5]. Here we show circularly-polarized THz wave emission from thin water flow irradiated by two time-separated and linearly-polarized femtosecond laser pulses. THz time-domain spectroscopy reveals the circularly-polarized THz emission dominates 4.7 ns after the first pulse irradiation. THz wave detection delay in the spectroscopy and time-resolved micrography indicate that the THz wave emission originates from the rarefied volume in front of the flow. Radial relaxation of charges (currents) in the focal volume where ponderomotive charge depletion occurred is the origin for the circular polarization; tight focusing localized THz wave emission to the sub-wavelength region.

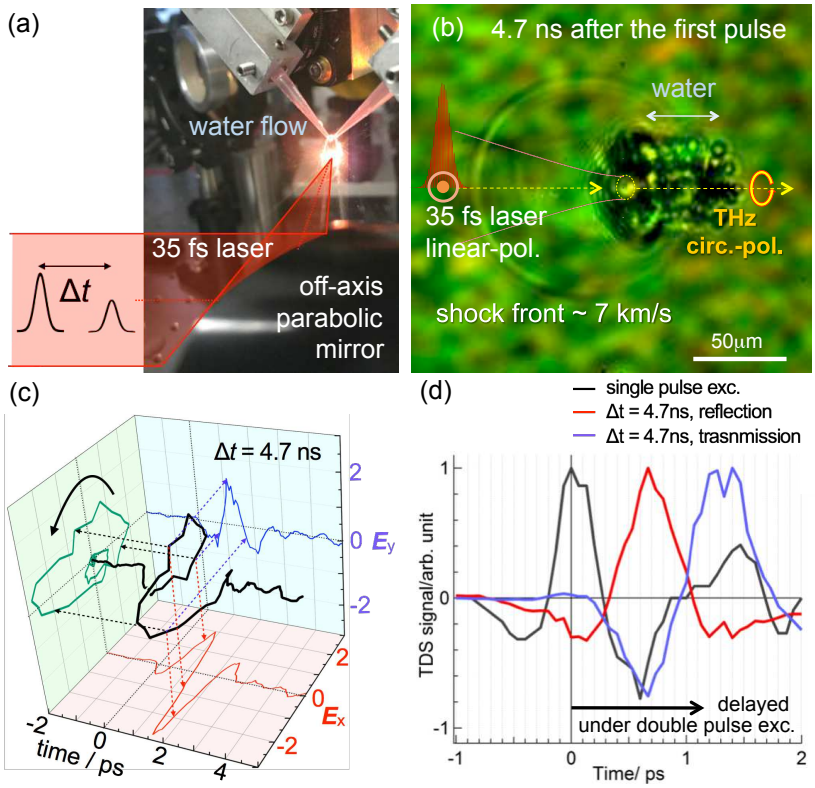

Fig. 1. Concept: tailoring the light-matter interaction for the polarization manipulation of THz wave. (a) A thin water flow irradiated by a pair of femtosecond laser pulses (35fs, 800nm) for THz wave generation. Pulses are tightly focused to a ~ 10 μm spot on the surface of a 17 μm-thick water flow. (b) Time-resolved shadowgraphy with ~ 1 ps temporal resolution; a representative photo captured at 4.7 ns after the first pulse irradiation. Details are in Suppl. S1.2 and Fig. S2. (c) Signals in THz time-domain spectroscopy (TDS) when the delay time at 4.7 ns, which indicates the circularly-polarized THz wave emission. Details are in Suppl. S1.1 and Fig. S1. (d) TDS time delay observed under the double pulse excitation; here TDS measurements were not polarization-discriminated.

(Introduction)

Creation of single-cycle THz wave sources and to control their polarisation could open a versatile toolbox of polarisation sensitive characterisation techniques currently developed at a rudimentary level. This study shows a promising direction towards generation of a single cycle circularly-polarised THz wave from focus of femtosecond laser pulse with sub-wavelength extension (for THz wave). Small sub-wavelength THz wave emitters provide flexibility in engineering THz wave sources with complex wavefronts, polarisation, and high power currently achieved by millimeters-long filaments [6].

THz wave ellipticity is important in the study of the physics of laser filamentation [7, 8], spin dynamics of solid state materials [9], chirality of proteins [10]. In material sciences, the state of angular momentum of light, i.e., its polarisation, effects the optical excitation [11], spectroscopy [12–14], and provides data transfer multiplexing in information technologies [15].

There are reports of circularly-polarized THz wave emission from plasma under a two-color

laser excitation [16–20]. The ellipticity of the THz wave can be controlled by the filament length with suitable input laser energy [21], the relative phase between the fundamental wave and the second harmonic pulses [22–24], the pulse energy [25], and changing the time delays between three-pulse configuration [26]. Polarisation of THz wave emission from the filament of optically induced plasma was described by considering a dipole radiation inside ~ 1 mm water jets [27,28] or in air [29] oriented along the propagation of femtosecond laser pulses and formed as a result of ponderomotive force. The ponderomotive force behind the ionisation front of a self-guided femtosecond laser pulse in air created a $L = 1 - 30$ cm long, ~ 0.1 mm diameter filaments which induced THz wave emission with a spatial intensity and polarisation pattern defined by a moving dipole mechanism [29]. The polarisation of THz wave emission was found to be linear-radial (in respect to the propagation axis) as revealed by the squared Malus dependence $\propto \sin^4\theta$. In this study, we investigate the case when the filament length, L, is sub-wavelength (sub-1 mm) at the tight focusing when L corresponds to the geometrical focus, i.e., the Rayleigh length (see, the concept illustration in Fig. 1). Tight focusing of ultrashort laser pulses has additional benefit for the higher THz wave emission due to scaling for the ponderomotive force induced wake field dipoles, $P_{THz} = \frac{1}{7}\left(\frac{E_p}{w_0}\right)^2\left(\frac{\lambda}{t_p}\right)^4$, where $w_0 = 0.61\lambda/NA$ is the waist of the laser beam at the focus (a lens with numerical aperture NA), t_p is pulse duration and λ is its wavelength [30]. THz wave emission from sub-wavelength filaments is not yet explored research area which is strongly required for ultimate control of intensity, direction, phase, and polarisation of THz wave sources.

Here, we report circularly-polarized THz wave emission from micro-thin water flow under double-pulse cross-linearly-polarized laser excitation. Axial extension of the THz wave-emitting filament of the second pulse (the main pulse) is enclosed inside the expanding water plume created by the first pulse (the pre-pulse) and has approximately the length of focal region of 60 μm at the focusing conditions. The most efficient THz wave emission corresponded to the pulse separation of 4.5-5 ns. A current generated to restore charge depletion along the optical axis due to action of the ponderomotive force with simultaneously occurring recombination between ions and electrons is 1-2 ps long defining the spectrum of THz wave emission. Detailed polarisation analyses of THz E-fields in the transmission and reflection directions are carried out by time-domain spectroscopy revealing peculiarities of sub-wavelength THz wave emission. The region of THz wave emission is also captured by time-resolved shadowgraphy/luminescence imaging experiments which confirm the origin of THz wave emission is in front, but not inside, of the water flow (Fig. 1).

(Results and discussion)

Figure 1(c) shows polarisation resolved emission of THz wave at the optimum conditions with delay between two pulses of 4.7 ns using time-domain spectroscopy (TDS); more details are described in Suppl. S1.1 with Fig. S1 where the $\boldsymbol{E}_x$ and $\boldsymbol{E}_y$ are measured in the transmission and the reflection directions. THz wave emission under the single pulse excitation maintains the same $\boldsymbol{E}_x$ polarization with the main pulse. However, under the double pulse excitation, THz wave emission changes its polarization from linear to circular as the delay time advances and its intensity reaches the highest at the delay time of 4.7 ns as reported previously without detailed polarisation analysis [5]. THz wave emission spectra obtained from TDS signals by discrete Fourier-transform, as shown in the inset in Fig. S1, show their peak shifts toward the lower frequency as the delay time increases. This indicates that the the interaction length of the main pulse E_2 with the ablated water plume after the pre-pulse E_1 irradiation becomes longer.

Figure 1(b) shows the time-resolved shadowgraphy image captured by back-side illumination of picosecond white light continuum at the maximum enhancement of THz wave emission. It clearly defines the geometry of the focal spot which is important in the estimation of light-matter conditions in the case on THz wave emission. The focus diameter on the flow was close to the

geometrical focus with the radius $\sim 0.61\lambda_l/NA \approx 4$ μm; $NA = 0.125$ is the effective numerical aperture of the off-axis parabolic mirror. This is markedly different from THz wave emission in self-guided filament formation in air ($\sim$ 100 μm diameter and centimeters-long) governed by self-focusing of femtosecond laser pulses [29]. Detailed evolution of micro-explosion is presented in details in shadowgraphs (Fig. S2 in Suppl. S1.2) revealing the evolution of the shockwave induced by the pre-pulse irradiation. Shockwave expansion velocity in air was approaching 7.6 km/s, which corresponds to strong explosion conditions. The radius of of the shocked hemisphere in front of the water flow is $R \approx 60$ μm (at the delay time of 4.7 ns) when the diameter of laser on the water is $w_0 \approx 8$ μm and depth of ablation is $h \approx 2$ μm. The additional ablated volume of water constitutes only 0.02% of volume in the shocked region, however, the molecular number density of water is 1.237×10^3 larger as compared with air. As a result, the molecular density of the water-air is at least by 26% larger as it is for the first pulse. This allows the plasma to reach higher density by the second pulse E_2. Indeed, as shown in the luminescence images (Fig. S2 in Suppl. S1.2), interaction of the main pulse with water flow previously modified by the pre-pulse irradiation becomes more dominant. The very central part of light-matter interaction on the flow surface is the source of X-ray emission since the electron temperature reaching $\sim$ 1 keV is achieved under the experimental conditions [4, 5] (see Suppl. S1.3; however, this study was solely focused on THz wave emission).

Figure 1(d) shows the time delay in TDS signals observed at the different excitation conditions. The TDS signals under the double pulse excitation delay for ~700 fs in the reflection and for ~1.4 ps in the transmission. By considering that the refractive index of water at 1 THz is $\sim$ 2.12 [31], it is consistent with direct imaging and indicates that the conversion from the near-IR laser to THz wave takes place in front of the original water flow surface. This observation indicates that the ablation of water by the pre-pulse E_1 and the shockwave dynamics is important for the THz wave emission under the double pulse excitation. The location of THz wave emission is presented earlier to originate from the inside of water flow [32] which is in this case highly unlikely due to extraordinary-high plasma density (water molecular density 3.35×10^{22} cm^{-3}) for the ponderomotive mechanism under employed intensity range.

Figure 2 shows the key features on the light-matter interaction relevant for the circularly-polarised THz wave emission. The second/main pulse E_2 ionises the outwardly fast expanding gas and the water vapor generated by the pre-pulse E_1. The most intense THz wave emission is observed at Δt =4.7 ns. This corresponds to the fast ($\sim$ 1 ps) currents along the optical path of the main pulse E_2, which are due to electrons and ions radially depleted along the propagation due to the ponderomotive force which for electron is $F_p = -\frac{e^2}{4m_e\omega^2}\nabla I$, where I is the laser intensity. The radial profile of the electronic density depletion on the axis of a Gaussian pulse $I(r) = I_0 e^{-4\ln 2(r/r_0)^2}$ is given by $N_e(r)/N_0 = 1 + \left(\frac{d^2}{dr^2} + \frac{1}{r}\frac{d}{dr}\right)\sqrt{1 + I^2(r)}$ where $N_{e,0}$ is the electron and background densities, respectively, r_0 is the FWHM of the focal spot. The radial electron displacement has a steeper gradient as compared with the axial charge separation due to ponderomotive force due to Gaussian intensity envelope. This is the key difference from the self-guided long filaments which never produced circularly-polarised THz wave emission since the radiating dipole (via Cherenkov-like mechanism) is axially oriented. The radial pattern of arrows in the xy-plane cross-section shows charge separation by the ponderomotive force (the radial pattern will occur for electrons, protons H^+ and O^+ which will have different radial distribution due to their difference in mass; see Suppl. S1.3). The radial ion-electron charge diffusion and recombination onto the optical axis takes place in the wake of the optical pulse. This ultrafast current transient is the source of THz wave emission which is phase-tailored into circularly-polarised radiation as the second pulse (35 fs or 10 μm) ionised the $\sim$ 60 μm long focal region. The current was initiated at the locations further away from the focus and propagated towards the water flow. It was shown that the circularly spiraling current will generate circularly-polarised THz radiation when spiral electrodes were used [33]. Previous studies with

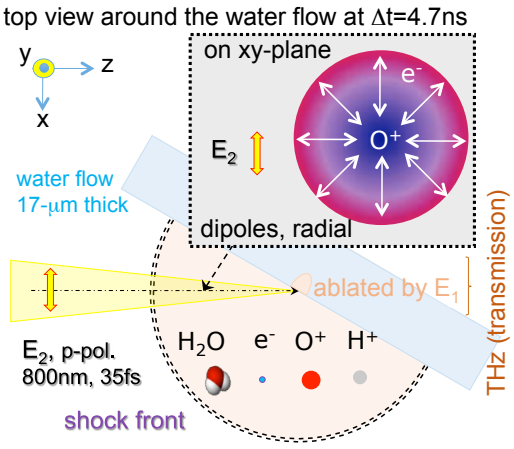

Fig. 2. Geometry of the experiment for the $NA = 0.125$ focusing depicted after the pre-pulse E_1 (y-pol.) irradiation to the water flow which creates the expanding plasma region out of the ablated water flow (strong explosion with shockwave of radius r_{sh}; see Suppl. S1.2). THz wave emission is induced by the current of ionised plasma rarefied along the center axis of the propagating E_2 laser pulse due to the radial ponderomotive force. The transient radial current $\partial J/\partial t$ is the source of THz wave emission. The Rayleigh length under the focusing conditions is $z_R \approx 60\ \mu$m ($2z_R$ is the depth-of-focus at 0.5-intensity level, i.e. FWHM), which would correspond to the $\lambda_{THz}/4$ for the emission at 1.25 THz (240 μm).

linearly-polarised light pulses have shown that in the case of irradiation of Ar cluster in vacuum by two time-separated pulses, the polarisation of the THz wave emission was defined along the line through the center of the first pulse and the position of the focus of the second pulse (which was shifted out of center by $\sim 40\ \mu$m) [34]. The intensity of the first pulse was inducing the charge depletion on the axis with positive ions closer to the center (on the optical axis). Electrons generated out-off-the-center by the second pulse caused a linear current (towards the center) and consequently linearly-polarised THz wave emission. The conditions of tight focusing explored in our study creates spatially confined plasma at the focal region along the optical axis. Since electrons, protons, and oxygen ions from the water flow (and oxygen and nitrogen from air) are separated radially to the different position by the pre-pulse, the second pulse initiates a spiraling current along the depth-of-focus (more details are discussed in Suppl. S1.4). The irradiation position of the first pulse to that of the main pulse is optimised for the strongest THz wave emission by the same methodology as we described earlier for the maximum of X-ray emission [5]; i.e., slight walk-off on the xy-plane is introduced for the maximum of the emission. This optimisation is obtained for approximately 10 μm shift along the x-axis on the flow surface. Quantification of the offset from the optical axis for the intensity and polarisation control of THz wave emission needs further studies. It is established in this study that the circularly-polarised single cycle THz pulse can be generated using the tight optical-focusing from ionised focal volume in the pre-plasma with the axial extent of $\lambda/4$ of THz wave emission.

(Conclusions and Outlook)

A simple two-laser pulse irradiation to a thin water flow is shown to generate circularly-polarized THz wave emission from a plasma filament which has length of approximately quarter wavelength of the THz emission (a sub-wavelength THz emitter). The mechanism responsible for the increased efficiency of THz wave emission as compared with the single pulse irradiation of

solid/liquid/gas targets is related to water ablation inside strong shock region in air in front of the water flow. The ablation condition for THz wave emission is optimal at the delay time 4.7 ns after the pre-pulse irradiation. The radial current transients restoring axially depleted charges due to action of ponderomotive force determines the spectral extent (a shorter transient broader spectrum as related via Fourier transform) and the circular polarisation of such THz wave emission. Circular polarisation is a result of radially spiraling currents which originate along the $\lambda_{THz}/4$ long Rayleigh region of optical focus (a linearly-polarised THz wave are observed from the axially oriented dipole in self-guided long filaments [29]). THz wave emission in the reflection and transmission directions in respect to the water flow has similar intensities but opposite polarisation. The transmission losses of sub-mm wavelength THz through 17-μm-thick water flow are slightly reducing the transmitted power. As previously reported [5], the highest intensity of THz wave emission from the water flow under the double pulse excitation is 10-times higher in $|\boldsymbol{E}|^2$ (as photon numbers) than that from a $\langle 110 \rangle$-oriented ZnTe crystal. Further enhancements are expected in other liquids such as gold nano-colloidal aqueous suspensions.

Circularly-polarised THz wave emission is adding new possibilities in a polarisation control toolbox for THz technologies which can open new applications for opto-mechanics where large torsion can be generated upon absorption, reflection, or scattering and for rotational/vibrational molecular spectroscopy where polarisation wave-plates are not readily available or lossy. THz wave can be used to better understand highly dynamic laser triggered explosions which find increasing number of application in laser machining/fabrication and creation of high temperature/pressure phases of new materials. Among different methods of electromagnetic field generation, sub-wavelength emitters are promising due to unmatched flexibility in wave front and polarisation engineering.

References

1. J. A. Fülöp, S. Tzortzakis, T. Kampfrath, Advanced Optical Materials **2020**, 8, 3 1900681.
2. I. Dey, K. Jana, V. Y. Fedorov, A. D. Koulouklidis, A. Mondal, M. Shaikh, D. Sarkar, A. D. Lad, S. Tzortzakis, A. Couairon, G. R. Kumar, Nat. Commun. **2017**, 8, 1 1184.
3. J. Qi, E. Yiwen, K. Williams, J. Dai, X.-C.Zhang, Appl. Phys. Lett. **2017**, 111, 7 071103.
4. H.-H. Huang, T. Nagashima, W.-H. Hsu, S. Juodkazis, K. Hatanaka, Nanomaterials **2018**, 8, 7 523.
5. H.-H. Huang, T. Nagashima, T. Yonezawa, Y. Matsuo, S. H. Ng, S. Juodkazis, K. Hatanaka, Applied Sciences **2020**, 10, 6 2031.
6. A. Koulouklidis, C. Gollner, V. Shumakova, V. Fedorov, A. Pugžlys, A. Baltuška, S. Tzortzakis, Nature Commun. **2020**, 11, 1 1.
7. L. Bergé, S. Skupin, C. Köhler, I. Babushkin, J. Herrmann, Phys. Rev. Lett. **2013**, 110 073901.
8. L. Bergé, J. Rolle, C. Köhler, Phys. Rev. A **2013**, 88 023816.
9. A. S. Prokhorov, V. B. Anzin, D. A. Vitukhnovskiĭ, E. S. Zhukova, I. E. Spektor, B. P. Gorshunov, S. Vongtragool, M. B. S. Hesselberth, J. Aarts, G. J. Nieuwenhuys, M. Dumm, D. Faltermeier, S. Kaiser, S. Yasin, M. Dressel, N. Drichko, Journal of Experimental and Theoretical Physics **2006**, 103, 6 887.
10. X. Yang, X. Zhao, K. Yang, Y. Liu, Y. Liu, W. Fu, Y. Luo, Trends Biotechnol. **2016**, 34 810.
11. T. L. Cocker, V. Jelic, M. Gupta, S. J. Molesky, J. A. J. Burgess, G. D. L. Reyes, L. V. Titova, Y. Y. Tsui, M. R. Freeman, F. A. Hegmann, Nature Photonics **2013**, 7, 8 620.
12. J. Zhu, Z. Ma, W. Sun, F. Ding, Q. He, L. Zhou, Y. Ma, Applied Physics Letters **2014**, 105, 2 021102.
13. B.-X. Wang, L.-L. Wang, G.-Z. Wang, W.-Q. Huang, X.-F. Li, X. Zhai, Applied Physics A **2014**, 115, 4 1187.
14. R. Singh, E. Plum, C. Menzel, C. Rockstuhl, A. K. Azad, R. A. Cheville, F. Lederer, W. Zhang, N. I. Zheludev, Phys. Rev. B **2009**, 80 153104.
15. S. Baierl, M. Hohenleutner, T. Kampfrath, A. K. Zvezdin, A. V. Kimel, R. Huber, R. V. Mikhaylovskiy, Nature Photonics **2016**, 10, 11 715.
16. D. J. Cook, R. M. Hochstrasser, Opt. Lett. **2000**, 25, 16 1210.
17. M. Kress, T. Löffler, S. Eden, M. Thomson, H. G. Roskos, Opt. Lett. **2004**, 29, 10 1120.
18. H. Zhong, N. Karpowicz, X.-C. Zhang, Applied Physics Letters **2006**, 88, 26 261103.
19. I. Babushkin, W. Kuehn, C. Köhler, S. Skupin, L. Bergé, K. Reimann, M. Woerner, J. Herrmann, T. Elsaesser, Phys. Rev. Lett. **2010**, 105 053903.
20. Z. Zhang, N. Panov, V. Andreeva, Z. Zhang, A. Slepkov, D. Shipilo, M. D. Thomson, T.-J. Wang, I. Babushkin, A. Demircan, U. Morgner, Y. Chen, O. Kosareva, A. Savel'ev, Applied Physics Letters **2018**, 113, 24 241103.
21. Z. Zhang, Y. Chen, S. Cui, F. He, M. Chen, Z. Zhang, J. Yu, L. Chen, Z. Sheng, J. Zhang, Nature Photonics **2018**, 12, 9 554.

22. H. Wen, A. M. Lindenberg, Phys. Rev. Lett. **2009**, 103 023902.
23. J. Dai, N. Karpowicz, X.-C. Zhang, Phys. Rev. Lett. **2009**, 103 023001.
24. Y. S. You, T. I. Oh, K.-Y. Kim, Opt. Lett. **2013**, 38, 7 1034.
25. Y. Chen, C. Marceau, S. Génier, F. Théberge, M. Châteauneuf, J. Dubois, S. L. Chin, Optics Communications **2009**, 282, 21 4283 .
26. H. Wang, N. Li, Y. Bai, P. Liu, Z. Wang, C. Liu, Opt. Express **2017**, 25, 25 30987.
27. X.-C. Zhang, F. Buccheri, Lith. J. Phys. **2018**, 58, 1 1.
28. E. Yiwen, Q. Jin, A. Tcypkin, X.-C. Zhang, Appl. Phys. Lett. **2018**, 113 181103.
29. C. D'Amico, A. Houard, M. Franco, B. Prade, , A. Mysyrowicz, A. Couairon, V. T. Tikhonchuk, Phys. Phys. Lett. **2007**, 98 235002.
30. H. Hamster, A. Sullivan, S. Gordon, R. W. Falcone, Phys. Rev. E **2007**, 98 235002.
31. J. Zhou, X. Rao, X. Liu, T. Li, L. Zhou, Y. Zheng, Z. Zhu, AIP Advances **2019**, 9, 3 035346.
32. Q. Jin, J. Dai, E. Yiwen, X.-C. Zhang, Appl. Phys. Lett. **2018**, 113 261101.
33. X. Lu, X.-C. Zhang, Phys. Rev. Lett. **2012**, 108 123903.
34. K. Mori, M. Hashida, T. Nagashima, D. Li, K. Teramoto, Y. Nakamiya, S. Inoue, S. Sakabe, Applied Physics Letters **2017**, 111, 24 241107.
35. H.-H. Huang, Y.-t. R. Chau, T. Yonezawa, M. T. Nguyen, S. Zhu, D. Deng, T. Nagashima, K. Hatanaka, Chemistry Letters **2020**, 49, 6 597.
36. P. Yeh, Optics Communications **1978**, 26, 3 289 .
37. F. Miyamaru, T. Kondo, T. Nagashima, M. Hangyo, Applied Physics Letters **2003**, 82, 16 2568.
38. N. Kanda, K. Konishi, M. Kuwata-Gonokami, Opt. Express **2007**, 15, 18 11117.

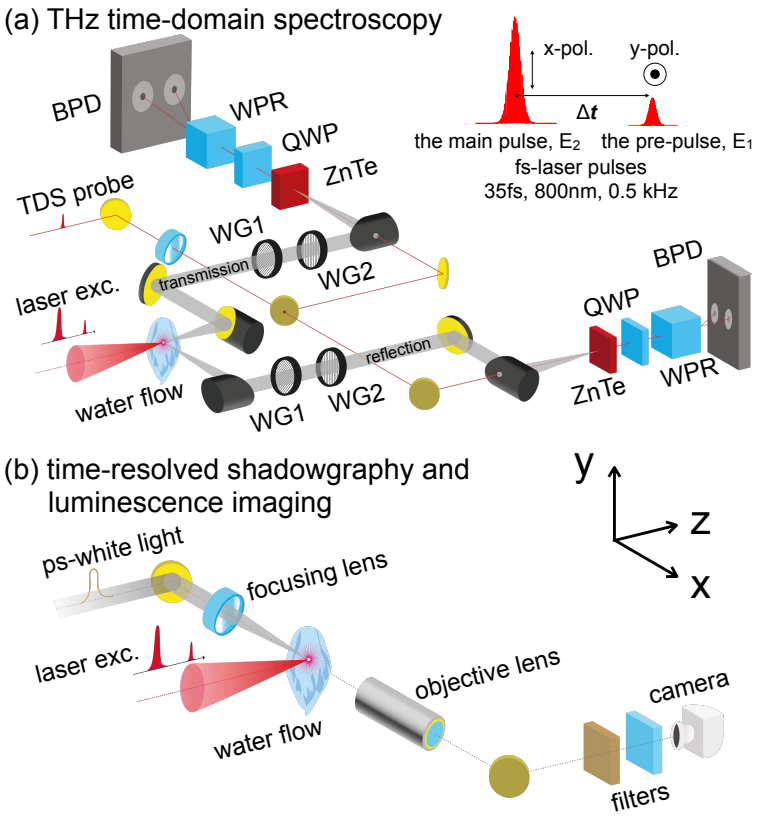

Fig. 3. Schematic diagrams of the experimental setups with the water flow (17 μm thick) under the tight focusing of double pulses with the pre-pulse (x-pol., E_1) and the main pulse (y-pol., E_2) (a) for THz time-domain spectroscopy (TDS) with a ZnTe crystal (for electro-optic sampling) and (b) for time-resolved shadowgraphy and luminescence imaging. Δt indicates the delay time between the two pulses. Polarization statuses of THz wave emission were measured with a pair of wire-grids. Imaging experiments for the laser focus were also carried out with an objective lens and a color camera with the exposure time at 2 ms for the single shot. The details are in the text. QWP:quarter wave-plate, WPR:Wollaston prism, BPD:balanced photo-diode

Methods

All the experiments shown in Fig.3 were carried out in air under atmospheric pressure (1 atm) at room temperature (296 K).

Polarization-sensitive THz time-domain spectrosocpy. A pulsed femtosecond laser (t_p = 35 fs, transform-limited, λ = 800 nm, 1 kHz, Mantis, Legend Elite HE USP, Coherent, Inc.,) is used and the output pulses are split into the pre-pulse (E_1, linearly-polarized parallel to y-axis, y-pol., 0.1 or 0.2 mJ/pulse), the main pulse (E_2, linearly-polarized parallel to x-axis, x-pol., 0.4 mJ/pulse), and the probe for THz time-domain spectroscopy (TDS) with a series of half-wave plates and polarization beam splitters (65-906, 47-048, Edmund Optics) as shown in Fig. 2 (a) [4, 5, 35]. THz wave emission is induced by the irradiation of the co-linearly combined pre-pulse and main pulse onto a thin water flow (~17 μm thick) by an off-axis parabolic mirror (1-inch diameter, effective focal length f = 50.8 mm, 47-097, Edmund Optics). The laser incident angle along z-axis is at 60° to the water surface normal. Under this condition,the polarisations of the main and the pre-pulses are p-pol. and s-pol., respectively. The optical delay between the two excitation

pulses, Δt, is controlled with automatic stages (SGSP46-800 and SGSP26-150, Sigma Koki). A water flow is prepared wth two colliding water jets and the system is set on an automatic stage (KS701-20LMS, Suruga Seiki) along the z-axis to adjust the flow surface for optimal X-ray emission measured by a Geiger counter (SS315, Southern Scientific). The detection of the THz wave emission is carried out by the electro-optic sampling method in the transmission direction through the water flow and in the reflection direction with ⟨110⟩-oriented ZnTe crystals (1-mm thick, Nippon Mining & Metals Co., Ltd.). Lock-in measurements are carried out with an optical chopper (3502, New Focus) and a lock-in amplifier (SR830, Stanford Research System), therefore the effective repetition rate of the laser excitation is 0.5 kHz. Following the usual method reported previously [36–38], two wire grids (WGs, MWG40FA-III, Origin) are additionally used for the measurements of polarization status in THz wave emission. One of the WGs, WG2, is used at the fixed angle 0°(parallel to x-axis), while the other WG, WG1, is used at two different angles, +45°and -45°for two independent TDS signals as $\boldsymbol{E}_{+45}$ and $\boldsymbol{E}_{-45}$, respectively. The x- and y-components of THz electric field, $\boldsymbol{E}_x$ and $\boldsymbol{E}_y$, are then calculated from $\boldsymbol{E}_x = \boldsymbol{E}_{+45} + \boldsymbol{E}_{-45}$ and $\boldsymbol{E}_y = \boldsymbol{E}_{+45} - \boldsymbol{E}_{-45}$, respectively.

Time-resolved imagings. Imaging experiments for the laser focus from the side (along x-axis) are also carried out in two different methods with an objective lens (M Plan Apo 10×, MITUTOYO) and a color CMOS camera (Blackfly S USB3, FLIR Systems, Inc.) with filters for IR-cut and for intensity control in the visible region. One is with the pre-pulse and white light continuum ($\sim$ 1 ps, 580 ± 30 nm, as a strobe light) converted from the main pulse with a water cell. With this method, transient refractive index changes and/or scattering due to pre-plasma formation and/or laser ablation induced by the pre-pulse irradiation can be visualized. Another imaging is with the pre-pulse and the main pulse, which visualizes the interaction of the main pulse with the water flow with structures prepared by the pre-pulse irradiation. The exposure time for the camera setting was fixed at 2 ms for single shot imaging. In this mode of image acquisition, all the emission in broad-band spectra by the two-pulse irradiation of the water flow is time-integrated.

Acknowledgments

S.J. is grateful for partial support by the ARC Discovery DP190103284, Linkage LP190100505 and JST CREST JPMJCR19I3 grants. T.N. is grateful for the support by JSPS KAKENHI Grant Number 20K05371. T.Y. is grateful for the support by Grant-in-Aid for Scientific Research for Fostering Joint International Research (B) (18KK0159). K. H. is grateful for the supports by the Ministry of Science and Technology (MOST) of Taiwan (107-2112-M-001-014-MY3), the Cooperative Research Program of "Network Joint Research Center for Materials and Devices", Nanotechnology Platform (Hokkaido University), and the Collaborative Research Projects of Laboratory for Materials and Structures, Institute of Innovative Research (Tokyo Institute of Technology). K. H. also acknowledges the Japan Science and Technology Agency (JST) PRESTO (Precursory Research for Embryonic Science and Technology) Program (SAKIGAKE, Innovative use of light and materials/life) for its supports on the original project on X-ray/THz wave simultaneous emission, "Ultrawide band light conversion by controlling structures of microdroplets and ultrashort laser pulse (2009-2013)" and for the laser facilities for the current project. H. -H. H. and K. H. acknowledge Mr. Yung-Jie Huang for his drawings of the experimental setups.

Figures

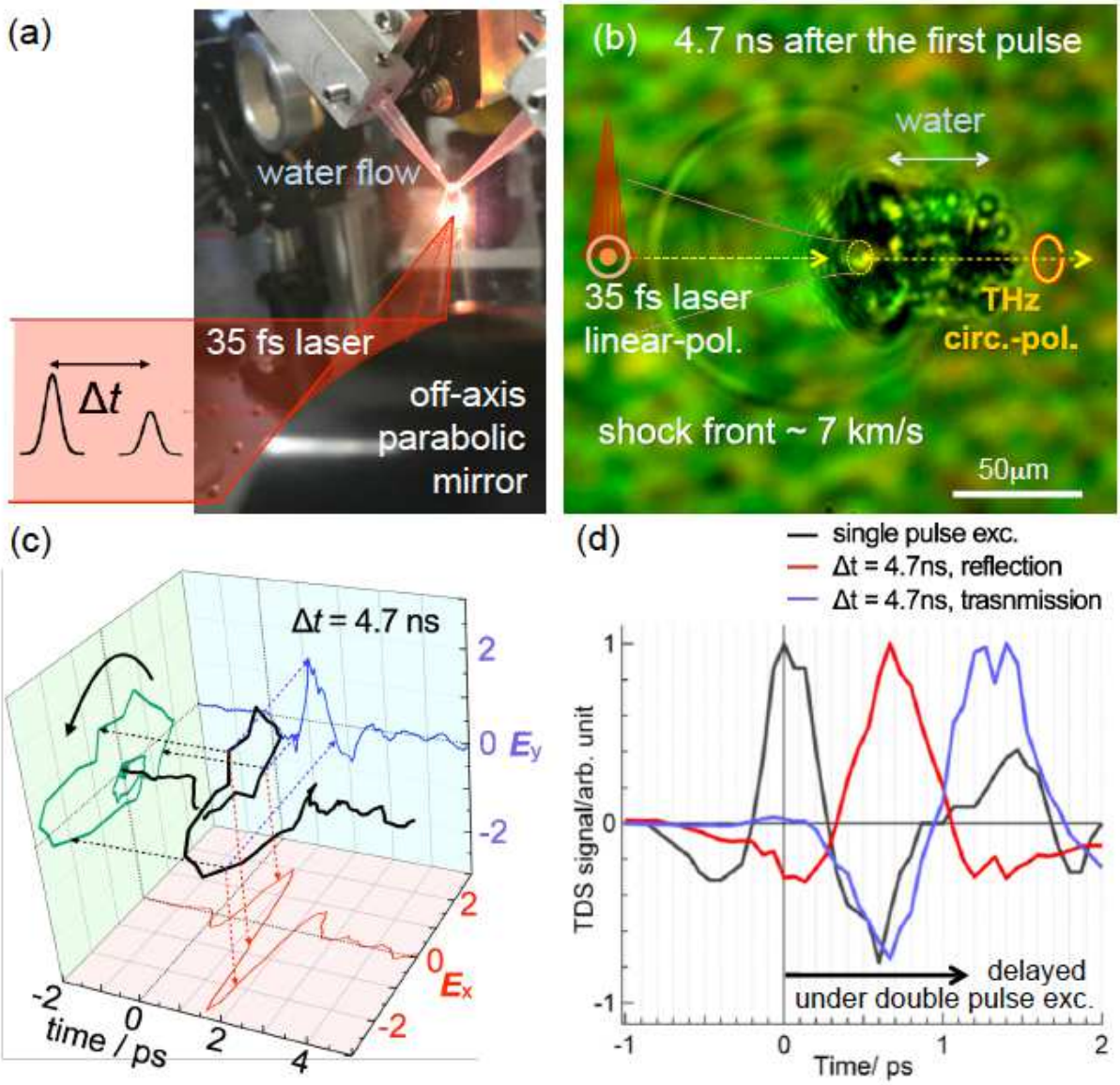

Figure 1

Concept: tailoring the light-matter interaction for the polarization manipulation of THz wave. (a) A thin water flow irradiated by a pair of femtosecond laser pulses (35fs, 800nm) for THz wave generation. Pulses are tightly focused to a ~ 10 μm spot on the surface of a 17 μm-thick water flow. (b) Time-resolved shadowgraphy with ~1 ps temporal resolution; a representative photo captured at 4.7 ns after the first pulse irradiation. Details are in Suppl. S1.2 and Fig. S2. (c) Signals in THz time-domain spectroscopy (TDS) when the delay time at 4.7 ns, which indicates the circularly-polarized THz wave emission. Details are in Suppl. S1.1 and Fig. S1. (d) TDS time delay observed under the double pulse excitation; here TDS measurements were not polarization-discriminated.

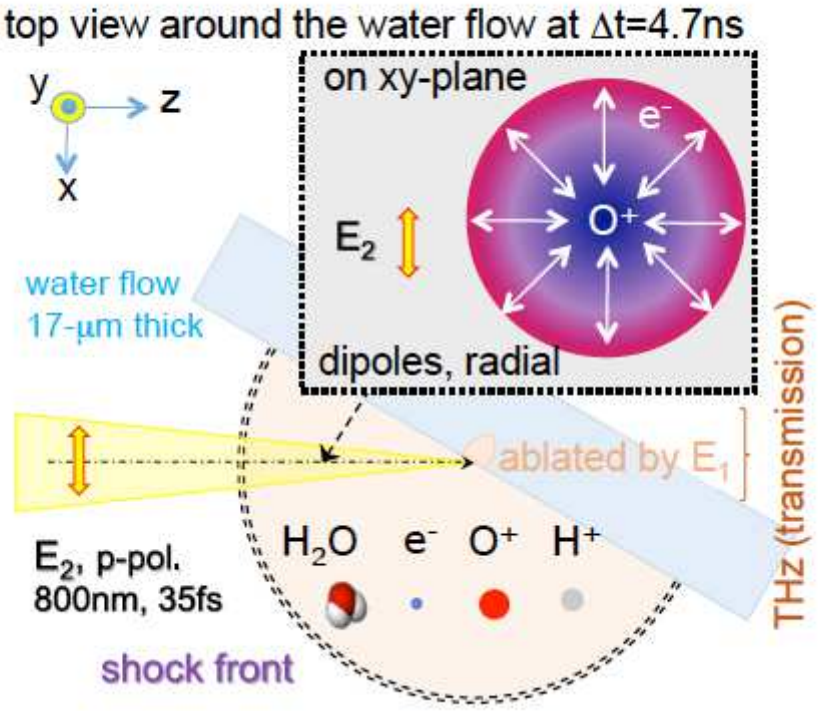

Figure 2

Geometry of the experiment for the NA = 0.125 focusing depicted after the pre-pulse E1 (y-pol.) irradiation to the water flow which creates the expanding plasma region out of the ablated water flow (strong explosion with shockwave of radiussh; see Suppl. S1.2). THz wave emission is induced by the current of ionised plasma rarefied along the center axis of the propagating E2 laser pulse due to the radial ponderomotive force. The transient radial current $\partial J/\partial t$ is the source of THz wave emission. The Rayleigh length under the focusing conditions is $z_R \approx 60$ μm ($2z_R$ is the depth-of-focus at 0.5-intensity level, i.e. FWHM), which would correspond to the $\lambda_{THz}/4$ for the emission at 1.25 THz (240 μm).

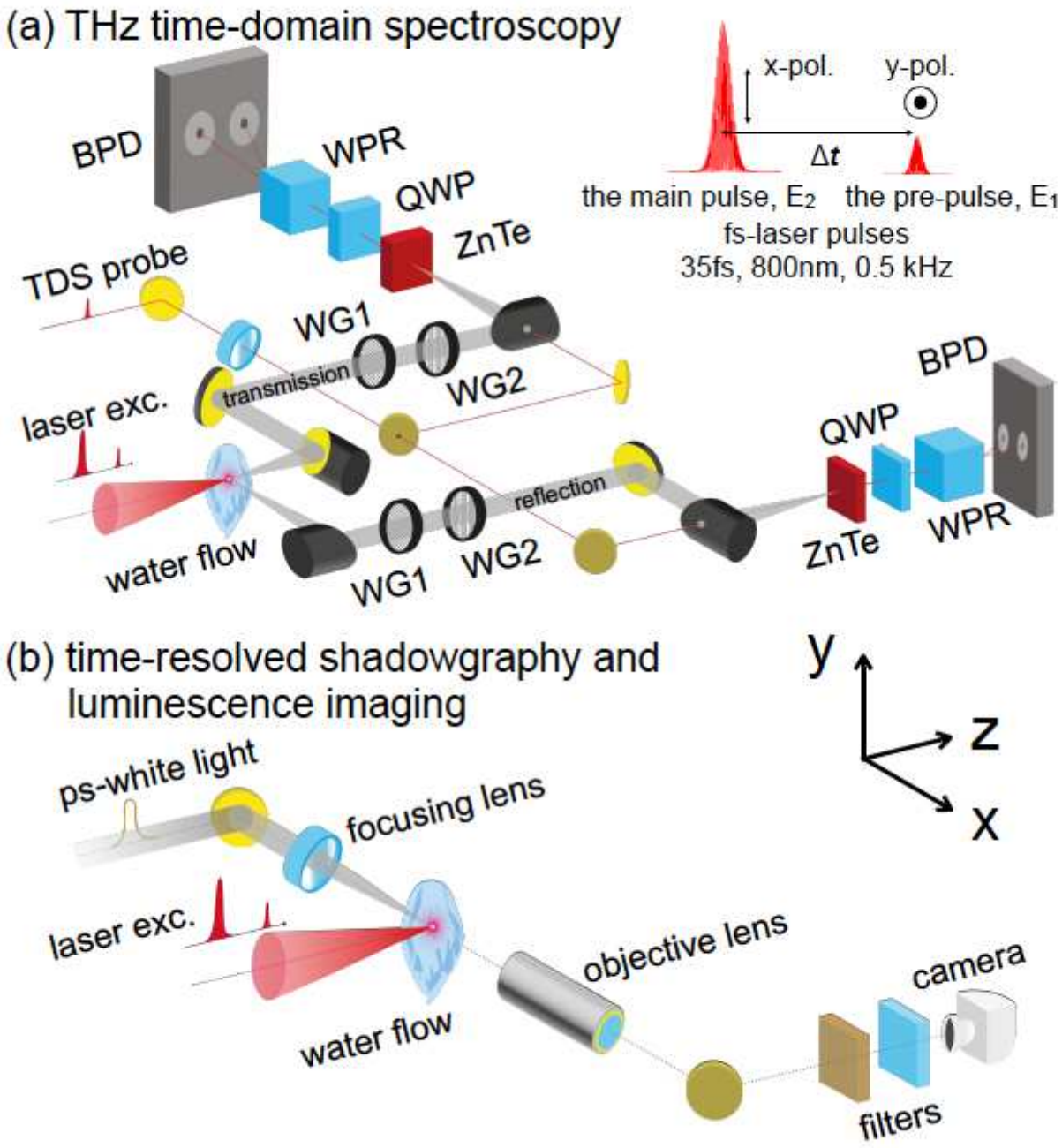

Figure 3

Schematic diagrams of the experimental setups with the water flow (17 μm thick) under the tight focusing of double pulses with the pre-pulse (x-pol., E1) and the main pulse (y-pol., E2) (a) for THz time-domain spectroscopy (TDS) with a ZnTe crystal (for electro-optic sampling) and (b) for time-resolved shadowgraphy and luminescence imaging. Δt indicates the delay time between the two pulses. Polarization statuses of THz wave emission were measured with a pair of wire-grids. Imaging experiments for the laser focus were also carried out with an objective lens and a color camera with the exposure time at 2 ms for the single shot. The details are in the text. QWP:quarter wave-plate, WPR:Wollaston prism, BPD:balanced photo-diode

Supplementary Files

This is a list of supplementary files associated with this preprint. Click to download.

- Supplement.pdf